Scramjet Combustion Processes

Michael Smart and Ray Stalker
Centre for Hypersonics
The University of Queensland
Brisbane 4072
AUSTRALIA

1.0 INTRODUCTION

Research into hypersonic flow phenomona has been conducted by numerous groups within Australia for over 40 years. The genesis of all the modern day work can be traced back to the return of the then Dr Ray Stalker from England, to take a faculty position in the Physics Department of the Australian National University, Canberra, in 1962. Dr Stalker had a keen interest in the aerodynamics of bodies travelling at speeds up to orbital velocity, and had devised a concept for generating such velocities in the laboratory through the use of a shock tunnel driven by free-piston compression. In the following years, Dr Stalker developed numerous facilities utilizing this concept, called free-piston shock tunnels, culminating in the commissioning of the T3 shock tunnel in 1968. A small group of researchers exploited the unique capabilities of T3, which was the first facility in which the product of test section density and model size, combined with the test section velocity, was such that the aerodynamic thermochemical phenomena generated at these elevated velocities were large enough to be measured. Bluff body shapes received early attention, as these shapes are typical of re-entry vehicles, and changes in the flow patterns due to dissociation thermochemistry were observed and analysed. Noting the interest in entry into the atmosphere of Mars, the bluff body studies were extended to include carbon dioxide flows, and because entry into the atmospheres of the large planets would involve ionisation, the effect of ionisation thermochemistry on bluff bodies was investigated. Dissociation thermochemical effects related to gliding re-entry vehicles also received attention, by studying the flow over an inclined flat plate, over a delta wing, and in the laminar boundary layer on a flat plate. The interaction of this boundary layer with a shock wave was also studied.

Sufficient experience had been gained with T3 by 1980 to begin research on scramjet engines, which offer the prospect of propelling an aircraft at these very high velocities. By this time Professor Stalker had taken a chair at The University of Queensland in Brisbane, and began leading a small group of researchers in pioneering work on the performance of scramjet engines at speeds in excess of 2.5 km/s. This team visited T3 for a number of weeks each year until 1987, when a larger shock tunnel facility known as T4 was commissioned at The University of Queensland. Since 1987 the primary mission of T4 has been to study combustion processes in scramjets. Scramjet models tested in T4 have progressed from simple generic models of a constant area combustor with a simplified fuel injector, to sophisticated models that involve the complete scramjet flowpath and flight vehicles.

This article describes some key aspects of the hypersonics research that has been performed at The University of Queensland. A short description of the operation of the T4 shock tunnel is followed by a discussion of some scramjet component research conducted in T4, and a description of research on complete scramjet flowpaths. A short summary of the HyShot 2 flight experiment is also included.

2.0 THE FREE PISTON SHOCK TUNNEL T4

T4 is shown in general arrangement in Fig. 1(a). A free piston is used to compress and heat the shock tube driver gas. A piston with a mass of 92 kg is normally used and, referring to the figure, is launched from the right-hand end of the compression tube, which is 26 m long and 228 mm in diameter, and initially

contains the shock tube driver gas. The piston is driven along the compression tube by the expansion of air initially contained in the piston driver reservoir, which has a volume of 1.2 m^3 and a maximum working pressure of 14 MPa. The piston acquires kinetic energy as it is driven along the compression tube, and this energy is then passed to the shock tube driver gas as the piston slows down on approaching the left-hand end of the compression tube. The driver gas is adiabatically compressed to pressures which are a multiple of the initial pressure in the piston driver reservoir. A high pressure diaphragm, located at the left-hand end of the compression tube, spontaneously ruptures when the shock tube driver gas reaches a predetermined pressure. This initiates conventional operation of the shock tube, which is 10 m long and 75 mm in diameter. The resulting shock wave in the test gas traverses the length of the shock tube and reflects from its left-hand end, where it ruptures a thin Mylar diaphragm to initiate the flow of test gas through the nozzle and test section. The shock heated test gas thus becomes the supply gas for the nozzle and test section flow, with a nozzle supply pressure which can somewhat exceed 50 MPa on a routine basis. This limit has recently been raised to 90 MPa.

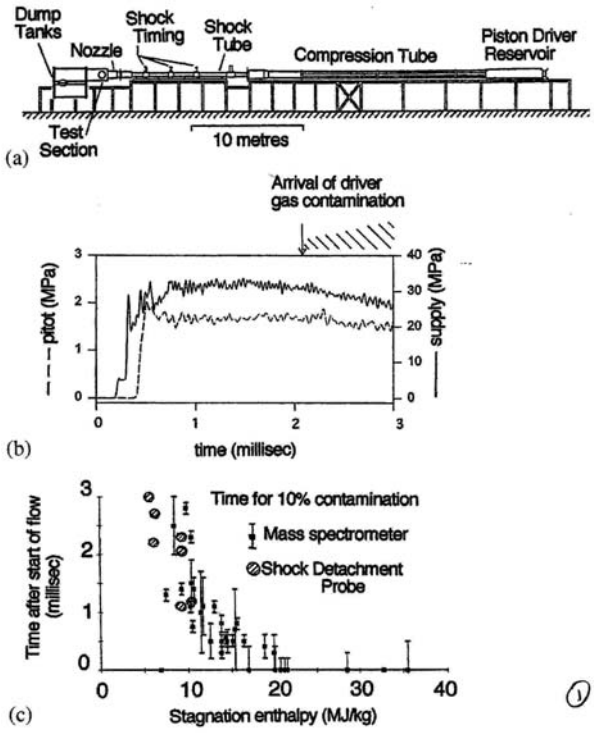

Figure 1: Free piston shock tunnel T4 at the University of Queensland: (a) general arrangement, (b) typical records of Pitot pressure, and nozzle supply pressure, (c) test time limit due to driver gas contamination.

2.1 Test Times – Driver Gas Contamination of the Test Flow

Typical records of test section Pitot pressure and nozzle supply pressure are shown in Fig. 1(b). A rule of thumb used in shock tunnel research is that the test flow must traverse three model lengths in order for the mainstream and boundary layer flows to effectively reach a steady state. The stagnation enthalpy of the figure (8MJ/kg) yields a flow velocity of about 3.5 km/s, indication that the flow would reach a steady state on a model 1 m long in 0.9 ms. Thus, the Pitot pressure record indicates that a steady-state flow persists for about 1.3 ms or 4.5 model lengths. However, the figure also shows the arrival of driver gas contamination of the test flow and, if the experiment in the shock tunnel demands uncontaminated test flow, then steady flow persists for only 0.5 ms, or 1.8 model lengths, and only test results obtained in this

time can be accorded unqualified acceptance. Thus, the useful test time in a shock tunnel may be determined by driver gas contamination, rather than by the time for which the nozzle supply pressure remained unchanged.

Measurements of the time to contamination in T4 arc presented in Fig. 1(c). The measurements were first made using a time of flight mass spectrometer (Skinner 1994), and later with a shock detachment probe (Paull 1996). The latter was developed as a simple instrument for routine monitoring of the test flow, and works by choking a duct when the specific heat of the flow gas increases beyond a critical value. It will be noted that the 10% contamination test time is reduced to zero for stagnation enthalpies in excess of 15 MJ/kg. It is thought that this may be due to turbulent mixing at the interface between the test gas and the driver gas in the shock tube. The peculiarities of the shock tunnel site demanded a length to internal diameter ratio of the shock tube of 133, instead of the value of 80-100 used in normal shock tunnel practice, and the extra length may have allowed extra mixing to take place. Notwithstanding this effect, it will be seen below that the test times available at stagnation enthalpies somewhat less than 15 MJ/kg have proven adequate for scramjet research.

2.2 Fuel Supply

Hydrogen fuel is used for almost all the tests performed to date, although both ethylene and gaseous kerosene have been recently used. Fuel is supplied to a model in the test section from a room temperature reservoir. For safety reasons, the capacity of the reservoir is limited so that if it were fully combusted in the test chamber it would reach a maximum working pressure of 10 MPa. The supply of fuel to the test section is controlled by a quick acting solenoid valve, which is slaved to the recoil of the compression tube to open and start fuel injection on the model approximately 10 ms before flow is initiated in the test section. Thus a constant rate fuel flow is established on the model before the test flow arrives. Fuel is injected through pre-calibrated orifices at the model, and the fuel flow is monitored by pressure transducers located as near to the injection orifices as is conveniently possible.

3.0 THE TWO-DIMENSIONAL COMBUSTION WAKE

The addition of fuel to a supersonic airstream in a duct, and the mixing and combustion which follows, will generate an increase in pressure along the duct. This pressure increase is at the heart of a scramjet, and leads to thrust generation in the expansion nozzle which follows the duct. To develop a knowledge of scramjets, it is important first to develop some understanding of the means of generating this pressure increase. This was done by studying combustion wake phenomena in relation to the pressure rise in a duct of rectangular cross section with a central injector spanning the duct, as shown in Fig. 2(a), to produce a flow which was essentially two-dimensional. The two-dimensional configuration was chosen because it offered relative simplicity for interpretation of experimental results, while recognizing that this configuration may not be the most efficient one in terms of providing maximum combustion in minimum combustion chamber length.

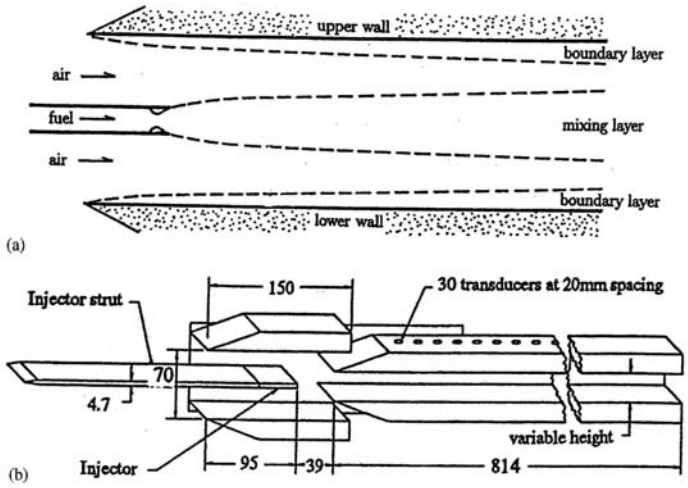

Figure 2: Combustion wake studies: (a) schematic of 2-D combustion duct, (b) typical experimental duct with side plate removed (dimensions in mm).

3.1 Wake Independent of Duct Height

The mechanism by which the duct pressure rise is produced was investigated experimentally using the configuration of Fig. 2(b) (Wendt et. al. 1999). The precombustion pressure in the duct was 61 ±5 kPa, the Mach number was 4.4±0.2, the stagnation enthalpy was varied from 5.6 to 8.9 MJ/kg and the associated air velocity varied from 2.9 to 3.5 km/s, while hydrogen fuel was supplied from a room temperature reservoir at a velocity of 2.3±0.1 km/s. Duct heights of 30, 50 and 70 mm were used, and the fuel flow rate was maintained at a value corresponding to an equivalence ratio of one with a 30 mm duct height.

The inset on the top right of Fig. 3 shows typical pressure distributions obtained when hydrogen fuel was injected into air and nitrogen. These were obtained under conditions corresponding to a precombustion temperature of 1480 K. The difference in the pressure distributions is ascribed to combustion, which clearly causes the fuel-air wake to produce a much greater pressure rise than the fuel-nitrogen wake. As indicated by the straight lines on the figure, the pressure increases linearly with distance downstream. Estimates of the ignition length for a hydrogen air mixture (Huber et. al. 1979) indicate that this length is less than an order of magnitude less than the length of the duct, indicating that the growth of the wake is governed by the process of mixing between hydrogen and air, rather than the reaction process.

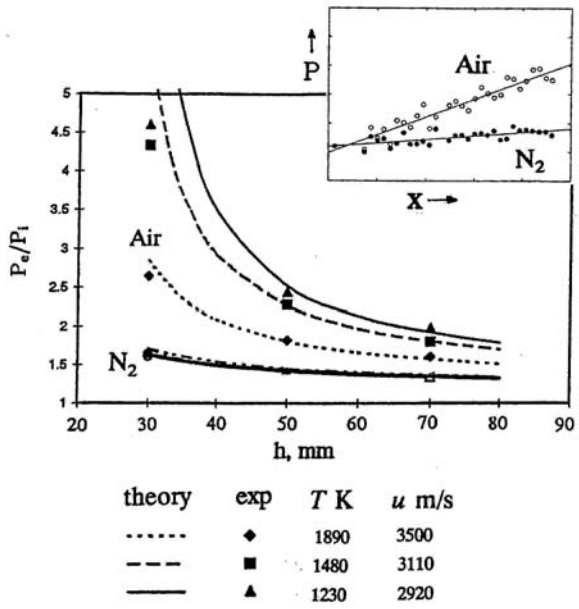

Figure 3: Displacement effect of combustion wake (Pe = exit pressure; Pi = precombustion pressure; x = distance from injector; h = duct height; T = precombustion temperature; u = precombustion air velocity).

A numerical analysis of this flow (Wendt et. al. 1999), based on the two-dimensional model of Fig. 2(a), found that the growth of the wake displacement thickness was responsible for the combustion induced increase in pressure along the duct and, the growth in displacement thickness was independent of the height of the duct. Figure 3 shows that, using the same combustion wake, a reasonable prediction can be made of the pressure rise along the duct by subtracting the sum of the displacement thicknesses of the wake and the boundary layers on the walls of the duct from the duct cross-sectional area, implying that as the duct height reduces, the mainstream experiences greater contraction and the pressure rise is increased. This model breaks down for the 30 mm duct at a temperature of 1230K, where it over-predicts the pressure rise but, for the less extreme conditions, it is possible to regard the development of the wake as decoupled for the associated pressure rise.

3.2 Scaling of Supersonic Combustion

Scaling studies are not only important for extrapolating from laboratory experiments to flight, but they can be helpful in revealing the dominant phenomena in a flow system. Experiments were done to compare the pressure distributions in the two ducts shown schematically in Fig. 4(a) (Pulsonetti 1997). To ensure the same composition of test gas entering the two ducts, the large duct was supplied with oblique shock recompressed flow from a Mach 8 shock tunnel nozzle and the small duct was supplied directly from a Mach 4 nozzle. The ducts were geometrically similar, but different in size by a factor of 5, the large duct height being 47 mm, and the small duct 9.4 mm. Precombustion pressures in the large duct varied from 25 to 10 kPa, and from 101 to 32 kPa in the small duct, while the precombustion Mach number was 4.4±0.2, and the hydrogen fuel equivalence ratio was 1.3±0.2.

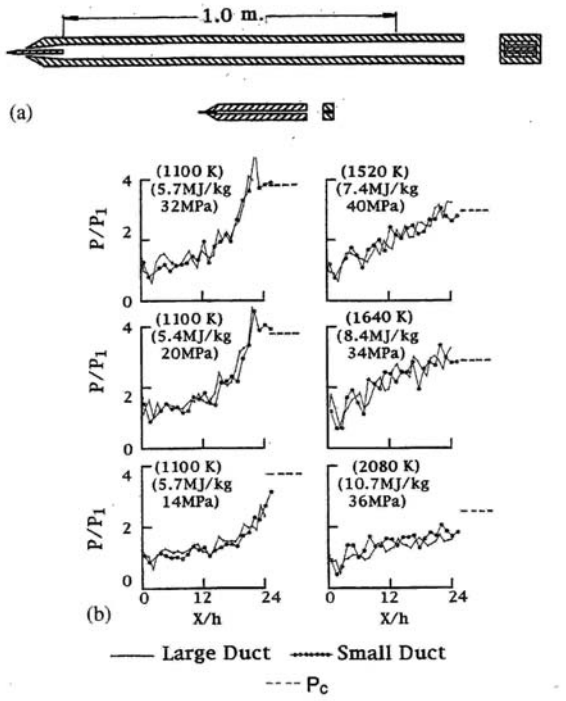

Figure 4: Scaling of supersonic combustion: (a) sketch showing relative scale of two combustion ducts, (b) pressure distributions (P_1 = precombustion pressure, P_c = theoretical peak pressure, x = distance from injector, h = duct height).

At each flow condition, the values of the product of the duct precombustion pressure and the duct height was the same for the two ducts. The results presented in Fig. 4(b) show that, by setting this product to be the same, identical normalized pressure distributions in the large duct and the small duct are obtained when the distance downstream of injection is scaled by the duct height. Thus, binary scaling applies to these flows, implying that small-scale experiments can be used as models of larger scale flows.

The pressure distributions on the right-hand side of the figure indicate the effect of varying the precombustion temperature while the precombustion pressure remains approximately constant, as indicated by the nozzle reservoir pressure on the figure. The linear pressure distributions, with the pressure gradient reducing as the precombustion temperature increases, indicate mixing controlled growth of the combustion wake, as in Fig. 3. It might be noted that Fig. 3 is also associated with linear pressure distributions at precombustion temperatures as low as 1230K.

The left-hand side of Fig. 4(b) indicates the effect of varying the precombustion pressure, as indicated by the values of nozzle reservoir pressure on the figure, while maintaining the precombustion temperature at 1100+/-50K. The gradient of the pressure rise along the duct is somewhat reduced as the precombustion pressure falls, but the most notable feature of these pressure distributions is that they do not exhibit the linear characteristic of those at higher temperatures. This non-linearity is consistent with the expected rapid increase in the flow length for reaction, which occurs as the mainstream temperature falls to about the temperature of these pressure distributions. At these temperatures the reaction length is sufficiently large that, in comparison with the mixing controlled flows on the righthand side of Fig. 4(b), the combustion release of energy is delayed, allowing more mixing and creation of radicals to take place, before a delayed but rapid energy release and relatively steep pressure rise. Thus, the pressure distributions on the left-hand side of Fig. 4(b) represent examples of reaction-controlled combustion.

Reaction-controlled combustion wakes were observed in other experiments. It was found (Casey et. al. 1992) that raising the precombustion pressure at a precombustion temperature of 1200K in the large duct would lead to the expected reduction in the combustion energy release delay but, as less mixing had then occurred, the combustion pressure rise was reduced. With a 25 mm duct height and precombustion pressures exceeding 150 kPa, the combustion energy release delay was further reduced (Stalker et. al. 1996), but the pressure rise was such as to suggest substantial combustion energy release and hence enhanced mixing. This may have been associated with the occurrence of a normal shock which was observed in the fuel rich part of the wake (McIntyre et. al. 1997). Other experiments (Buttsworth 1994) have shown that the interaction between a shock wave and a wake can lead to enhanced mixing.

An approximate combustion pressure rise may be calculated by using a Rayleigh analysis (Hall 1951), with the square of the Mach number much greater than one both before and after the heat addition zone, to yield

$$p_c / p \approx 1 + (\gamma - 1)\Delta Q / a^2 \qquad (1)$$

where p_c = downstream pressure, ΔQ =combustion heat release, a = speed of sound and γ = ratio of specific heats.

Equation 1 with ΔQ = 3.45 MJ/kg and γ = 1.3 provides an estimate of the resultant pressure levels if all the oxygen in the air entering the duct is burnt, and this level is shown in Fig. 4(b) for each pair of pressure distributions. The duct lengths are just sufficient for complete combustion, except at the highest pre-combustion temperature, where it is expected that the combustion energy release was limited by partial dissociation of the combustion products.

4.0 FORCE MEASUREMENT

After a significant series of component experiments, some of which have been described here, Prof. Stalker and the group at The University of Queensland began to experiment with complete scramjet configurations. These involved the integration of the inlet, combustion duct and thrust nozzle into one complete model. The obvious measurement to initially make on such models is the net thrust (or drag) as this is the essential measure of installed scramjet performance. Such measurement demanded the development of a new shock tunnel measurement technique.

In the shock tunnel, flow is initiated and forces are rapidly applied to the model, causing stress waves to occur that will, by reflection and re-reflection, traverse the length of the model many times before the model comes into stress equilibrium. It follows that the few flow model lengths of test time available in a sub-orbital shock tunnel were, in general, not sufficient for the model to come into stress equilibrium, and therefore that the overall forces acting on a model could not be measured by available force balance methods, since these treated the model as a rigid body.

Fortunately, the stress waves which were the source of this difficulty can themselves be exploited to measure the force on the model. This is done by placing strain gauges on the model support system and recording the time history of the strain produced by the stress waves passing into the supports. Deconvolution of the strain records then would yield the forces on the model. For measurement of the thrust or drag of a slender body, supported from a downstream sting, a single strain gauge, recording the strain time history of stress waves passing into the sting, would yield a satisfactory measurement.

The relation between the strain measured in the sting, u(t), and the axial force on the model y(t), can be described by the integral:

$$y(t) = \int_0^t G(t-\tau)u(\tau)d\tau \qquad (2)$$

where G(t) is a pre-determined impulse response function, and t and τ are time. The impulse response function can be determined numerically or by experiment, for example, by measuring the strain history resulting from application of a sudden increase in axial load on the model. The deconvolution of the integral of eqn. 2 to yield the axial force history, u(t), from the recorded strain history, y(t), is accomplished by a numerical procedure using a personal computer.

The method was first applied to measurement of the drag on a relatively short cone, with 15° semi-vertex angle (Sanderson & Simmons 1991). In this case, the internal stress waves in the model were unimportant, but the stress wave balance was established as a viable method of measuring axial force. Subsequent measurements of drag were made on a 5° semi-vertex angle cone which was 425mm long (Tuttle et. al. 1995, Tuttle 1996), where the internal stress wave reflections were significant, and yielded results consistent with theoretical estimates. The sensitivity of the method to the distribution of drag producing forces on the model was investigated numerically during this project leading to the conclusion that measured drag was independent of the force distribution on the cone.

The numerical investigations just referred to included a case where the drag force was concentrated at the tip of the cone. The fact that this did not influence the measured drag was exploited to conduct an investigation of the effect of nose blunting on the drag of a 5° semi-vertex angle cone (Porter et. al. 1994). The tests were done at a stagnation enthalpy of 15 MJ/kg with a test flow in which driver gas contamination occurred, but was less than 30% of the test flow by molar concentration. It was found that the drag remained at a constant value when the radius of the blunt nose remained less that 0.12 times the radius of the base of the cone. This indicates that a moderate degree of nose bluntness could be used to accommodate nose tip heat transfer effects on scramjet inlets without directly affecting the drag.

The stress wave force balance has also been used with a two-dimensional straight thrust nozzle in an exercise aimed at determining the influence of skin friction on thrust (Tuttle 1996). The nozzle had plane sidewalls, was 300 mm long and 54 mm wide, and had two thrust surfaces which were symmetrically disposed about the nozzle center-line, each with a divergence angle of 11°. The nozzle was supported by a two sting system, and was otherwise freely suspended immediately downstream of a fixed combustion duct, which supplied flow to the nozzle. Provision was made for fitting the thrust surfaces with transducers. Thus, the measured net thrust could be compared with the thrust obtained from measured pressure distributions to assess the thrust loss due to skin friction. It was found that this thrust loss was 20% +/- 5% of the pressure thrust, and was consistent with approximate estimates using a skin friction coefficient of 3×10^{-3}. These estimates indicated that approximately half the skin friction drag was associated with the nozzle walls, and therefore the skin friction drag on the thrust surfaces was roughly 10% of the pressure thrust. However, the presence of combustion in the combustion duct did not measurably affect the skin friction drag, indicating that the combustion thrust increment, obtained by subtracting the fuel-off pressure thrust from the fuel-on pressure thrust, is not measurably affected by skin friction.

The stress wave balance method was extended to simultaneously measure three components of force (Mee et. al 1996), and was used for experimental measurement of the lift, drag and pitching moment on a 15° semi-vertex angle cone 220 mm long, at angles of incidence which varied from 0° to 5°. Results were consistent with theoretical calculations, and led to use of the three-component stress wave balance for scramjet experiments.

5.0 INTEGRATED SCRAMJET FORCE MEASUREMENTS

With the development of the stress wave balance for measuring axial force, it became possible to measure the thrust/drag performance of integrated scramjet configurations. The axisymmetric scramjet model shown in Fig. 5(a) was chosen for initial experimentation (Paull et. al. 1995). The model is shown with half the cowl removed. It consisted of an axisymmetric center-body, with six combustion chambers and associated intakes arranged about its periphery. These intakes consisted of compression ramps formed by the splitters which separate the combustion chambers.

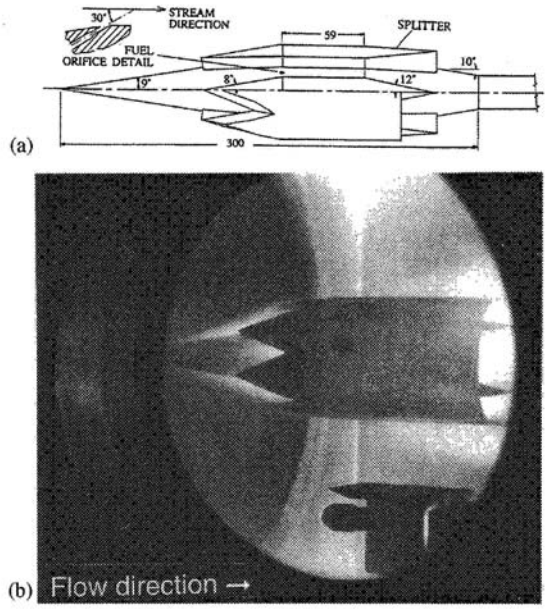

Figure 5: Integrated scramjet model: (a) model details (dimensions in mm), (b) time integrated photograph of model (3MJ/kg).

5.1 Model Design

Experiments with integrated scramjet configurations are more demanding of shock tunnel performance than the component experiments described so far. This is illustrated in the design of the scramjet model. In order to avoid the possibility of thermal choking at the lower end of the sub-orbital velocity range, a post combustion Mach number of approximately 2 was chosen which, with a constant area combustion duct and a heat release corresponding to stoichiometric combustion of hydrogen, implied a precombustion Mach number of approximately 4. This Mach number is a result of the inlet compression process. For a scramjet in atmospheric flight, where the static temperature is fixed, it would be necessary for the inlet compression process to yield precombustion temperatures and pressures which are high enough to assure ignition and burning of the fuel but, because the shock tunnel can supply an airflow at any reasonable freestream temperature, the temperature requirement can he relaxed. The function of the scramjet inlet compression process in a shock tunnel is therefore to raise the precombustion pressure to a suitable multiple of the freestream pressure. Choosing a value of 10 for this multiple, representing a reasonable thermal cycle efficiency, and an inlet compression process which took place through three oblique shocks, resulted in a freestream Mach number of 6 and an inlet contraction ratio of 4.8. Detailed intake considerations reduced the inlet contraction ratio to 4.4. The thrust nozzle expansion ratio is, through geometrical considerations, related to the inlet contraction ratio and, with the value of the inlet contraction ratio just quoted, the expansion ratio of the thrust nozzle was 5.8.

The value of the precombustion pressure must be sufficient for the combustion reaction and associated heat release to take place. For the hydrogen air reaction, Fig. 4 indicates that the value of the product of precombustion pressure and combustion chamber length should be approximately 15 kPa m. The length of the combustion chamber, at 0.06m, was limited by the model size, which was itself limited by the shock tunnel test time, and this combustion chamber length led to a required precombustion pressure of 250 kPa. Unfortunately, the shock tunnel nozzle supply pressure was limited to 40 MPa for these experiments and, with a freestream Mach number of 6, the precombustion pressure was limited to 100kPa. Thus the limitation of the shock tunnel nozzle supply pressure led to a precombustion pressure which was insufficient to sustain complete hydrogen air combustion. Or, to put it another way, the demands made by this integrated scramjet experiment exceeded the shock tunnel performance levels.

However, by using hydrogen fuel mixed with silane (SiH_4) as an ignition promoter, it was possible to reduce the pressure required for combustion. The results of central injector constant area combustion duct experiments with hydrogen-silane fuel mixtures (Morris 1989) indicated that, at the expected minimum scramjet model precombustion temperature of 800 K, the required value of the product of precombustion pressure and combustion chamber length was approximately 3 kPa m with a fuel mixture which included between 20% and 5% of silane by molar concentration. Assuming that, as with hydrogen fuel, the mode of injection would not significantly affect the combustion lengths, it was concluded that a fuel consisting of 13%, silane and 87% hydrogen would undergo complete combustion heat release within the combustion chamber length at a precombustion pressure of 100 k Pa.

Relatively large increases in pressure occur through the inlet compression process, and the boundary lavers must be able to negotiate these pressure increases without separation. Therefore, the Reynolds numbers on the forecone of the model should be high enough to ensure transition to a turbulent boundary layer. A study of transition on a flat plate in the shock tunnel (He and Morgan 1994) had yielded a transition Reynolds number which varied from 2.5×10^6 to 1.0×10^6 as the stagnation enthalpy increased. The corresponding forecone Reynolds numbers were 2.7×10^6 to 1.2×10^6 over the same range of stagnation enthalpies and this, together with the disturbances to the boundary layer generated by the compressions shocks, indicated that transition to a turbulent boundary layer would occur on the forecone. Figure 5(b) shows the scramjet model in operation in the shock tunnel. Flow luminosity on the forecone arises from flow compression by the conical shock formed on the forecone. The absence of the regions of high luminosity which would be associated with the strong shock waves resulting from choking is an indication that the inlet compression process is performing as designed. The high luminosity seen at the downstream end of the cowl is associated with the combustion region, and is thought to be due to silicon released during the combustion process.

5.2 Performance of the Model

The performance of the scramjet model in shock tunnel tests is presented in Fig. 6 in terms of the net thrust Coefficient, C_{TN}. Two continuous lines are displayed, with associated experimental points, showing the comparison between experimental and theoretical values of the axial force, both with fuel injection and without fuel injection. The theoretical values were obtained by adding the calculated inviscid and viscous axial forces acting on the inlet, combustion chambers and the thrust nozzle. The consistency between the axial forces calculated in this manner and the measurements served as a check on the validity of the calculation. Fig. 6 also displays two broken lines. The lower one on the figure represents the fuel off drag, and is fitted by eye to the associated experimental points. This broken line was used to yield values of the drag coefficient, C_D, for the upper broken line, which was obtained from theoretical calculations of the forces on the engine. These calcuations yield values of the net thrust coefficient which are generally consistent with the experimental results, with a tendency to somewhat underpredict the drag at stagnation enthalpies exceeding 4 MJ/kg. A positive thrust was obtained only at stagnation enthalpies below this level.

At stagnation enthalpies below 3.0 MJ/kg, unsteadiness in the thrust began to appear, and attempts to increase the thrust, either by further lowering the stagnation enthalpy or by increasing the fuel equivalence ratio led to choking of the scramjet inlet. This is unlikely to have been due to thermal choking of the combustion chambers, as eqn. 1 indicates that insufficient heat release is taking place, so the choking is attributed to boundary layer separation in the engine due to the combustion pressure rise.

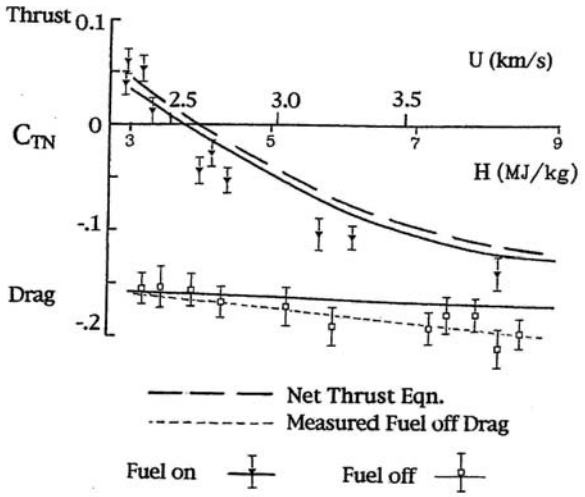

Figure 6: Performance of the axisymmetric scramjet model in the shock tunnel (U = velocity, H = stagnation enthalpy).

5.3 Hydrogen Fuelled Scramjet Models

The use of a silane-hydrogen mixture as fuel did indeed reduce the value of the pressure x combustion chamber length parameter required for essentially complete combustion, but it also increased the mixture molecular weight with respect to hydrogen, and therefore had the disadvantage that it reduced the fuel specific impulse. In an attempt to show experimentally that this reduction could be avoided, a scramjet model was designed in which combustion of hydrogen fuel would be encouraged, without the need for an ignition promoter (Stalker & Paull 1998). Figure 7 shows detail of one half of the model, which was symmetrical about the plane AA' in the figure. This symmetry was necessary because, at the time the experiments were done, the force balance could only operate with axial loads. An inlet contraction ratio of 5.2 was used, with the aim of producing a local region of high temperature and pressure and, to minimize choking tendencies when combustion occurred, was followed by a divergent combustion chamber. Hydrogen fuel injection took place at the minimum cross-section. It was found that, although the model flow started and ran during the shock tunnel test time with no fuel injection, the flow choked when the fuel flow was initiated before the shock tunnel flow, but ran when the fuel flow was initiated after initiation of the shock tunnel flow. A possible explanation for the choking effect may he that the injected fuel interacted with the shock tunnel nozzle starting flow to establish a choked flow which was subsequently maintained by combustion. Using the delayed fuel injection technique, it was possible to establish a steady flow with hydrogen combustion.

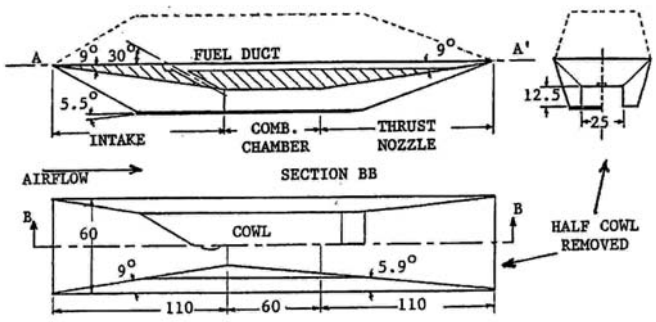

Figure 7: Hydrogen fuelled scramjet cruise model (dimensions in mm).

In experiments at a stagnation enthalpy of 3.5 MJ/kg and a Mach number of 6.4, the thrust with combustion increased with equivalence ratio, and became equal to the drag as the equivalence ratio approached unity, thus achieving the cruise condition of net zero thrust or drag. By comparison with results of pressure measurements in a combustion duct thrust nozzle combination, it was conceded that combustion was taking place in the thrust nozzle (Stalker et. al. 2004, Stalker & Paull 1998) but as indicated by a measured fuel specific impulse of 835 seconds, a portion of the fuel did not burn. Thus, although the use of an ignition promoter had been avoided, the fuel specific impulse of hydrogen fuel had not been fully realized. It is worth noting that the fuel off drag coefficient was 0.183, which is similar to the drag coefficient of the axisymmetric scramjet model discussed above, and was again divided approximately equally between inviscid and viscous drag.

6.0 INLET INJECTION AND RADICAL FARMING

The integrated scramjet force measurements indicated that mixing and combustion of hydrogen could not be completed at the precombustion pressures and combustion duct lengths of the experiments in section 5. Not only did this limitation lead to development of the shock tunnel to increase operating pressure levels, but it also encouraged experiments on two concepts; one designed to reduce combustion duct lengths for complete combustion, and the other to explore a mode of combustion different from the diffusion flame modes considered so far.

The first of these concepts involved injection of fuel on the inlet. Inlet injection has clear advantages in allowing mixing of hydrogen with air at the relatively low temperatures of the inlet before the mixture enters the combustion duct and ignites, thereby ensuring that the combustion process in the combustion duct is not delayed by the necessity for mixing. However, it was important to ensure that ignition did not occur prematurely, and thereby cause drag on the inlet due to the resulting combustion pressure increase. Experiments involving surface pressure measurements and shadowgraph flow visualization were done with injection through surface orifices in the inlet. The scramjet walls were at room temperature and the stagnation enthalpy was 3.0 MJ/kg (Gardener 2001). No evidence of inlet combustion was detected, but combustion was observed in the combustion duct. Experiments were also done with hydrogen injected through orifices in an inlet surface which was heated to 500 K (Kovachevich et. al. 2004), and no evidence of inlet combustion was detected either by surface pressure measurements or by interferometric imaging.

The second concept combined inlet injection with a technique to promote early ignition of the fuel-air mixture called “radical farming” (Odam 2004). This technique is illustrated in Fig. 8(a), which represents a two-dimensional scramjet configuration. The shocks or compression waves which make up the inlet compression process are arranged to form a local region of elevated pressure and temperature, near the entrance to the combustion duct, where the production of the chemical radicals, which are a first stage in

the overall combustion process, will be encouraged. This region is called the radical farm, and is isolated from the walls of the combustion duct by a lower pressure, cooler flow. The radical farm is terminated by the expansion waves from the corner at the combustion duct entrance, but the radicals remain "frozen" in the flow until they meet another region of elevated temperature and pressure, where combustion continues. The benefit of radical farming is that, because of the exponential dependence on temperature of the rate of radical formation, the regions of elevated temperature and pressure in the radical farms provide accelerated development of the ignition process.

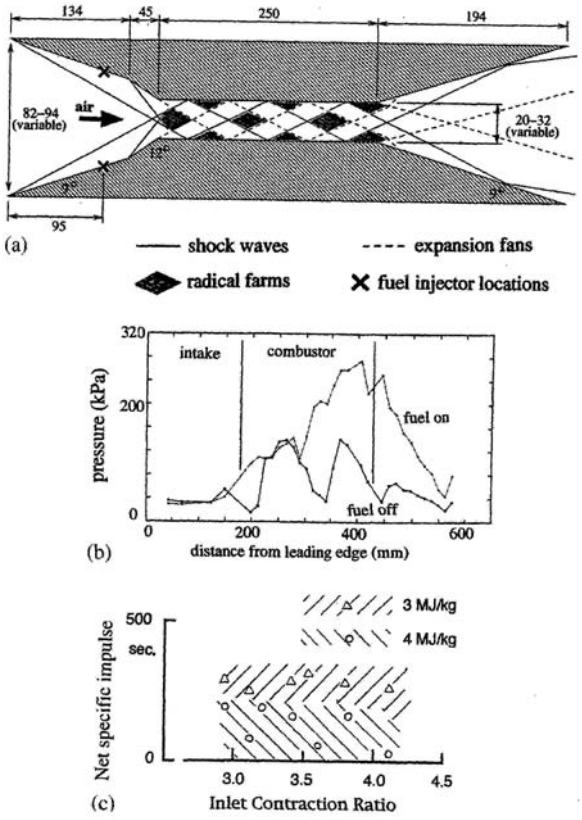

Figure 8: Experiments on radical farming (dimensions in mm).

Experiments were done with the two-dimensional configuration of Fig. 8(a). The model was 75 mm wide, and was fitted with sideplates to ensure two-dimensional flow. Pressure measurements were taken in the model midplane, along the inlet, combustion duct and thrust nozzle, together with measurements along three transverse lines to check that the flow was two-dimensional. Typcial pressure distributions are displayed in Fig. 8(b), and show that vigorous combustion occurred within the length of the combustion duct. Using the inlet flow conditions, a mean precombustion temperature of 700 K is obtained for the case of Fig. 8(b), a temperature which has been found to be too low for combustion in other experiments with constant area combustion ducts. Thus radical farming offers considerable improvement in the ignition characteristics of a hydrogen-fuelled scramjet.

Integration of the measured pressure distributions was used to obtain a two-dimensional inlet drag and nozzle thrust, and this was combined with skin friction calculations for all interior surfaces (including the interior of the side plates) to obtain an interior flowpath net thrust. Using measured values of the injected fuel mass flow, this net thrust could be converted to a net specific impulse, which is presented in Fig. 8(c). The inlet contraction ratio was varied by adjusting the spacing between the upper and lower halves of the

scramjet model, as shown in Fig. 8(a), and at each contraction ratio, the equivalence ratio was increased until choking occurred. At a stagnation enthalpy of 3 MJ/kg, the equivalence ratio for choking fell from 0.65 to 0.35 as the contraction ratio was increased from 2.9 to 4.1 and at 4 MJ/kg, it fell from 0.85 to 0.40. Estimates indicated that, as the contraction ratio changed, the radical farms persisted without major changes in their dimensions, suggesting that combustion processes in the model were essentially independent of the contraction ratio. This is in contrast to the more conventional scramjet, where the inlet contraction ratio determines the precombustion temperature, which strongly influences the combustion process. Fig. 8(c) confirms this independence by presenting points which were obtained by taking the mean of 2-4 measurements of the net specific impulse near the choking limit at each value of the contraction ratio. As represented by the cross-hatched zones, the net specific impulse values tended to remain constant as the contraction ratio was varied at both the stagnation enthalpies tested, indicating that combustion heat release was not significantly affected by the changes in contraction ratio. It may also be observed that the net specific impulse values, though small, are all positive, indicating that positive net thrust was obtained for the internal flowpath of this scramjet model.

7.0 SKIN FRICTION REDUCTION BY BOUNDARY LAYER COMBUSTION

The importance of skin friction drag in reducing the net thrust with an integrated scramjet configuration focussed attention on a means of reducing skin friction in turbulent boundary layers. Noting that the Reynolds stresses in a turbulent boundary layer play the role of viscosity, and that they are density dependent, it was thought that they could be reduced by raising the temperature, thus reducing the effective viscosity. In addition, the reduction in density would increase the width of the boundary layer streamtubes, and these two effects of increasing the boundary layer temperatures would both tend to reduce the skin friction.

This concept was tested by doing experiments with the rectangular duct configuration shown in Fig. 9(a) (Goyne et. al. 2000) at a stagnation enthalpy of 7.8 MJ/kg and a pre-injection pressure, temperature and Mach number of 50 kPa, 1500K and 4.5, respectively. Hydrogen was injected from a room temperature reservoir, at a Mach number of 1.8, through a slot at the wall which spanned the 100 mm dimension of the duct cross-section. Thus, the flow over the surface downstream of the slot was nominally two-dimensional. As shown in the figure, this surface was instrumented to measure pressure and heat transfer, while four skin friction gauges were used to measure skin friction at the indicated station. The height of the duct was such that combustion could be confirmed by an increase in the pressure rise along the duct length. Results from the experiments are presented in Fig. 9(b) for an injected hydrogen mass flow of 0.40 kg/s per metre width of the slot. Large reductions in skin friction are apparent for hydrogen injection and combustion, with the skin friction coefficient then only one quarter of the skin friction coefficient with no injection. To confirm that this effect was due to combustion, experiments were done with nitrogen test gas under the same test conditions. Although the figure shows a reduction in skin friction, due to the reduction in boundarv layer densities caused by hydrogen mixing, the reductions in skin friction are much less than when combustion of the injected hydrogen took place. Figure 9(b) also displays heat transfer measurements showing that near fuel injection, the Stanton number with fuel injection is much less that the Stanton number without fuel injection and rises towards no injection values well downstream. This reduction in heat transfer takes place in spite of the combustion heating of the boundary layer. It occurs because, by virtue of Reynold's analogy, the reduced skin friction coefficient implies a reduced Stanton number, and this effect is only partially offset by the additional combustion related heat transfer close to injection. Further downstream, more of the injected hydrogen is burned and combustion heat release has a greater relative influence on heat transfer.

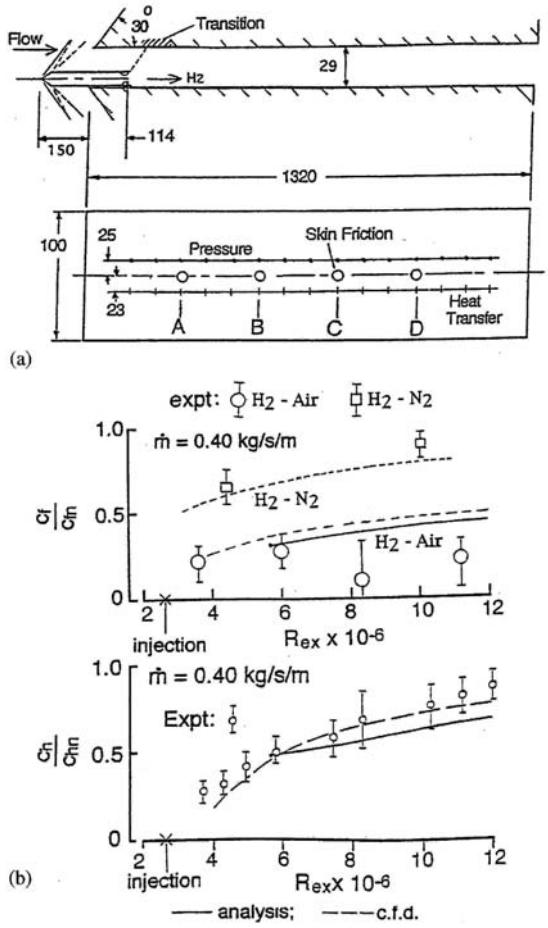

Figure 9: Turbulent skin friction reduction by boundary layer combustion; (a) Experimental duct details (dimensions in mm); (b) skin friction and heat transfer measurements (C_f,C_{fn} = skin friction coefficient with and without hydrogen injection, C_h, C_{hn} = Stanton number with and without hydrogen injection, $\dot{m}$ = hydrogen mass flow).

The experimental results in Fig. 9(b) were compared with predictions of a numerical simulation (Goyne et. al. 2000, Brescianini 1993) and a theoretical analysis (Stalker 2005). The numerical simulation employed finite rate chemistry, a κ–ε turbulence model, a parabolic Navier-Stokes code, and assumed a uniform pressure over the surface on which the boundary layer was formed. It was generally consistent with the experimental results in predicting a reduction in skin friction in the absence of hydrogen combustion, and a large reduction in the skin friction with combustion. The low values of measured skin friction coefficient at the two downstream stations are thought to be an effect of the pressure gradients along the wall acting on the reduced wall friction. The combustion induced heat transfer reduction was also predicted satisfactorily.

The theoretical analysis (Stalker 2005) used a model of the turbulent boundary layer formulated by Van Driest, which represents the effect of temperature induced density changes in the boundary layer on the skin friction on a flat plate. The Van Driest model was extended by incorporating the changes in temperature and density resulting from the injection of hydrogen along the surface from an upstream slot. Combustion of the hydrogen with oxygen was assumed to take place instantaneously when the two came into contact, regardless of the temperature. This allowed the distribution across the boundary layer of the species mass fractions and the stagnation enthalpy to be determined by using the Shvab-Zeldovich scheme

for coupling of these variables. The density could then be obtained as a quadratic relation in the boundary layer velocity, as in the analysis of Van Driest, but with coefficients which were different to those of Van Driest. This expression was used to yield the momentum thickness, which was differentiated with respect to the downstream distance to obtain the skin friction. As shown in Fig. 9(b), this analysis yields results which are in approximate agreement with results from the numerical simulation and the experiments.

The analysis has been employed to determine the effect on skin friction and heat transfer on a flat plate for flight velocities up to 6 km/s. It yielded values of skin friction drag which were less than half of the fuel-off skin friction drag, together with a net reduction in heat transfer when the combustion heat release in air was less than the stagnation enthalpy. The mass efficiency of hydrogen injection, as measured by effective specific impulse values was approximately 2000 seconds. Clearly, if boundary layer combustion of hydrogen can be realized over a sufficiently wide range of freestream conditions, it can be an important factor in increasing penetration of integrated scramjet configurations into the sub-orbital regime.

8.0 THE HYSHOT 2 FLIGHT EXPERIMENT

The ultimate test of shock tunnel predictive capability is a direct comparison of shock tunnel data with data obtained in flight with the same experimental configuration and the same flow conditions. Although examples existed where fight data for external aerodynamics was compared with shock tunnel data (Krek & Stalker 1992), flight data involving supersonic combustion did not exist in the late 1990's, thus eliminating the possibility of a comparison with shock tunnel data. However, this situation changed when two sounding rocket flights became available to The University of Queensland for supersonic combustion experiments.

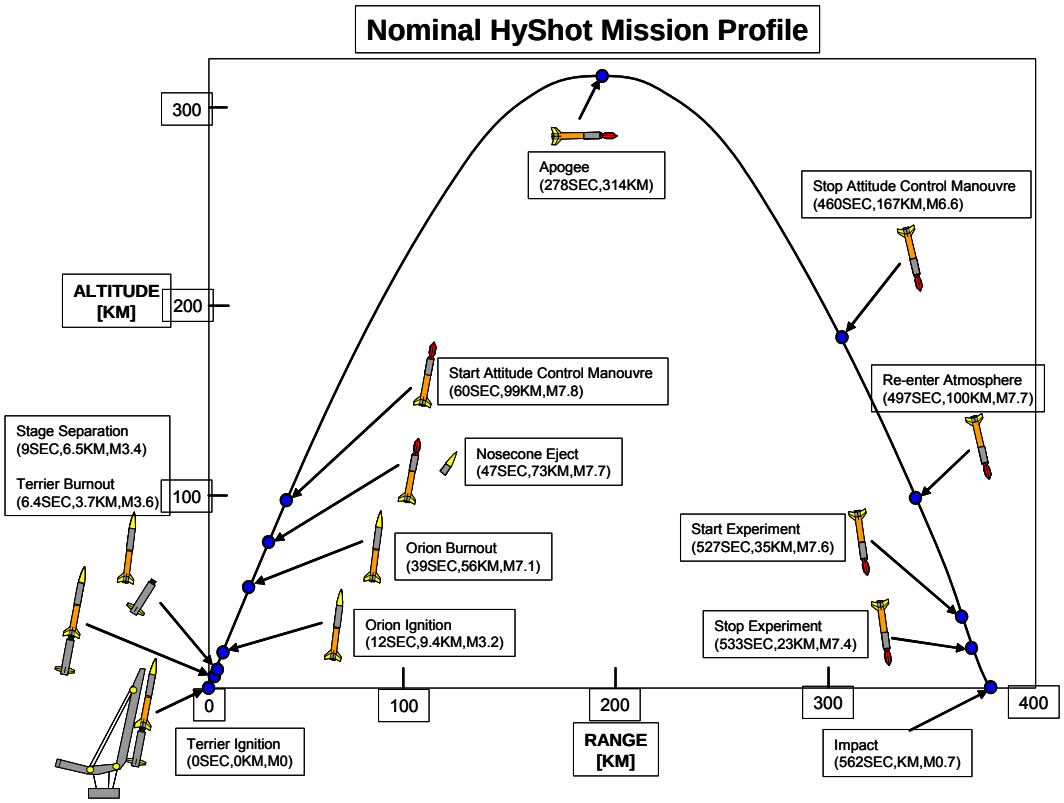

Figure 10: HyShot flight profile.

The sounding rockets were two-stage Terrier-Orion combinations, and were supplied by Astrotech Space Operations Inc. of the USA. As shown in Fig. 10, the flight began with ignition, followed by burnout and separation of the Terrier first stage, and subsequent ignition and burnout of the Orion second stage. The burnt out Orion remained attached to the experimental payload, in order to provide aerodynamic stability on re-entry to the atmosphere. The resulting flight vehicle then followed a parabolic trajectory, ascending to an altitude of 314 km before descending towards the atmosphere. While executing this manoeuvre, a control jet was activated in a "bang-bang" mode to realign the flight vehicle so that it re-entered the atmosphere with the experimental model pointing downwards. Re-entry was accomplished with a steep trajectory, allowing the experiment to take place over a planned period of 7 seconds as the vehicle passed from 35 km to 23 km in altitude (Paull et. al. 2002, Smart et. al. 2006).

A photograph of the experimental model is shown in Fig. 11, with a schematic of the fuelled flowpath in Fig. 12. The aim of the experiment was to establish a correlation between the conditions for supersonic combustion of hydrogen fuel in the shock tunnel and in flight, and the experiment was therefore designed to be a simple as possible. A two-dimensional flow configuration was chosen, consisting of two identical flow paths, symmetrically disposed about the center-line, both of which were instrumented for pressure measurement. By arranging that fuel was injected into only one of the two combustion ducts, it was possible to compare fuel-on with fuel-off pressure distributions, and thus to make a flight to shock tunnel comparison of the effect of the hydrogen fuel mixing and combustion processes.

Figure 11: HyShot 2 payload.

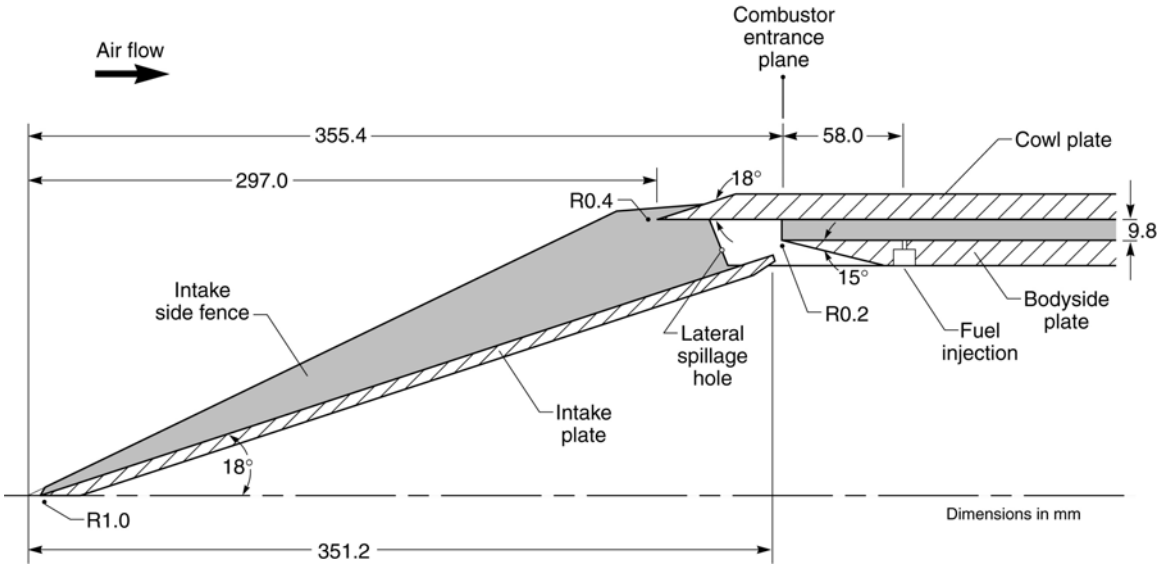

Figure 12: Schematic of fueled flowpath in the HyShot 2 payload.

The inlet consisted of a single 18 deg. wedge with a width of 100mm, a blunted leading edge, and highly swept side fences. The high wedge angle was necessary to ensure that the combustor entrance temperature and pressure were great enough to readily induce self-ignition of hydrogen. The rectangular combustor had a constant area 9.8 mm x 75 mm cross-section and a length of 300 mm (length/height = 30.61). The combustor cowl spanned the full width of the intake wedge and was situated such that the intake shock was upstream of its leading edge at all times. The flowpath design incorporated a shock trap that was situated between the end of the inlet wedge and the entrance of the combustor. This feature not only captured the cowl shock, but also bled off the intake boundary layer. The reduced width of the combustor (relative to the inlet wedge) and lateral spillage holes in the side fences adjacent to the shock trap, were designed to remove the fence boundary layers and corner flows. The angle-of-attack of the payload was defined as positive when the fuelled combustor was on the windward side, and negative when the fuelled combustor was leeward.

The flight produced a significant set of scramjet combustor data at varying duct entrance pressure, temperature and Mach number. Trajectory reconstruction was accomplished using onboard sensors alone (Cain et. al. 2004). Fuel flow was initiated at approximately t = 536.5 seconds after launch as the payload and attached Orion motor re-entered the atmosphere. Figure 13 shows the Mach number and dynamic pressure time histories during three seconds of the experimental window and Table 1 lists four zero-yaw time slices used for analysis. Figure 14 shows a comparison of the fuelled and unfuelled combustion pressure distributions at windward conditions: i.e. when each combustion duct was at a positive angle-of-attack of approximately 5 degrees. Note that all data is normalized by the combustor entrance pressure, in order to make meaningful comparisons. The equivalence ratio of the fuelled duct was approximately 0.34, and the pressure rise from combustion of the hydrogen fuel is clearly evident. Cycle analysis of this data indicated that supersonic combustion occurred at these times slices during the flight, at a combustion efficiency for the fuel of 81%.

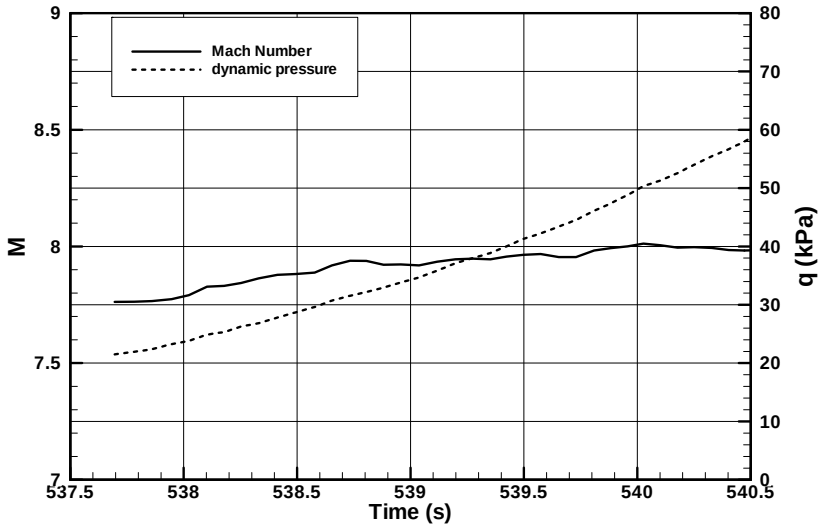

Figure 13: Reconstructed Mach number (M) and dynamic pressure (q) histories.

Table 1: Flight parameters for analyzed time slices.

number	Time (s)	Flight Mach Number	Flight dynamic pressure (kPa)	Altitude (km)	angle-of-attack(deg.)
1	538.103	7.828	24.88	34.48	-5.012
2	538.179	7.831	25.33	34.31	5.540
3	538.734	7.938	31.55	33.05	-5.081
4	538.805	7.938	32.20	32.89	4.617

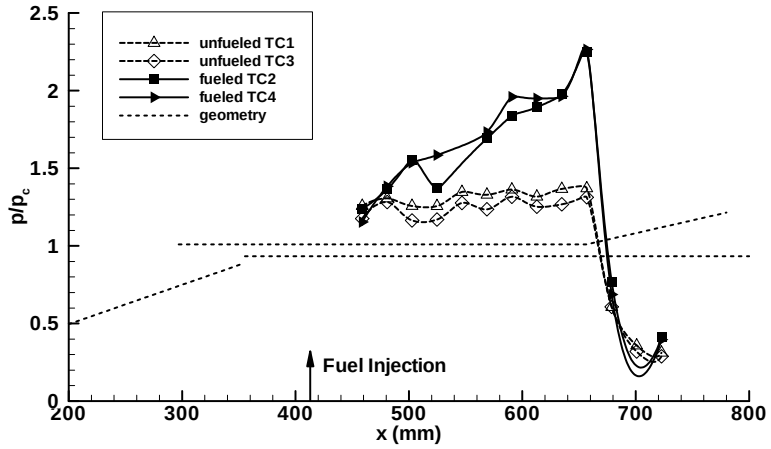

Figure 14: Windward fueled and un-fueled combustor pressure distributions (p = duct pressure, p_c = combustor entrance pressure, x = axial distance from nose of payload).

One of the important motivations for the HyShot flights was validation of short duration ground testing for scramjet development. As a first step towards this, a series of pre-flight experiments were conducted at The University of Queensland in the T4 shock tunnel to determine the expected performance of the flight payload. These experiments were documented in Paull et. al. (2000), and four of these shock tunnel runs are compared here with the presented flight time slices.

The model used for the pre-flight ground tests was designed to generate similar combustor entrance conditions to flight at Mach 7.6, while using an existing Mach 6.5 shock tunnel nozzle. This dictated the use of an experimental model with a 17^o wedge intake (compared to 18^o in the flight payload) and shock tunnel nozzle exit conditions with higher freestream pressure and temperature than flight. The 300 mm length combustor and fuel injectors were identical to flight, except that fuel injection took place 40 mm downstream of the combustor entrance (compared to 58 mm in flight), and the ground test model had an increased number of combustor pressure taps. A final difference between the ground and flight hardware was that the nozzle expansion was situated on the bodyside of the combustor in the ground test model (compared to the cowlside for the flight hardware).

Figure 15 shows a comparison between ground and flight data for the fuelled combustor at windward conditions. Both ground and flight data showed a clear pressure rise due to supersonic combustion of hydrogen, and Fig. 15 confirms that both ground and flight had similar pressure distributions along the combustor. It is interesting to note, however, that despite the fact that the ground data had a higher equivalence ratio than flight (0.47 compared to 0.34), both ground and flight generated very similar normalized pressure levels up to the last pressure tap in the ground model. Additional ground experiments are planned with a model and test conditions identical to the flight experiment.

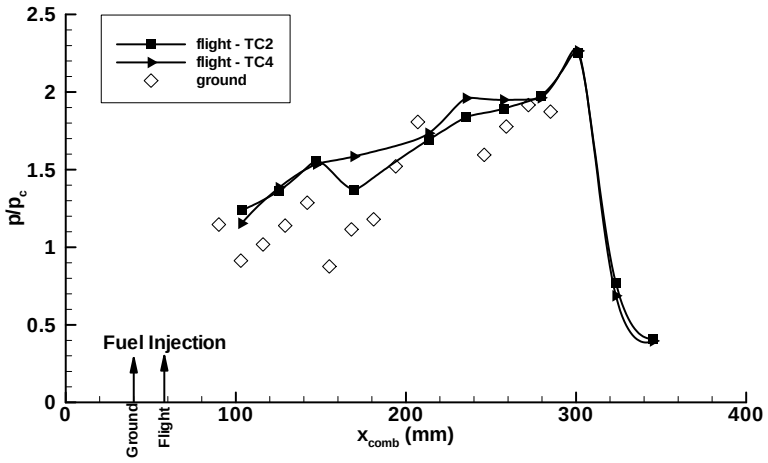

Figure 15: Flight-to-ground comparison at windward conditions.

10.0 FUTURE PLANS

Hypersonics research in Australia is alive and well. The success of the HyShot flights has led to a significant interest in low cost scramjet flight-testing using sounding rocket boosters. In November 2006, an agreement was signed between the Defence Science and Technology Organisation (DSTO) of Australia and the United States Air Force, to support a 10-flight test program called HIFiRE. The goal of this program is to develop the technology required for long duration scramjet flight at Mach 8. The University of Queensland is responsible for the payloads to be flown on three of the ten flights; designated HyShot 5, 6 and 7. The plan for these flights is as follows:

HyShot 5 – A Free-Flying Hypersonic Glider

HyShot 5 will be a hypersonic glider designed to fly at Mach 8. It will separate from its rocket booster in space and perform controlled manoeuvres as it enters the atmosphere. This flight will not have a scramjet attached. Both an up-and-down trajectory similar to HyShot 2, and a more horizontal "depressed" trajectory are being considered for the flight. The goal of the flight is to learn about the control of hypersonic vehicles in the upper atmosphere.

HyShot 6 – A Free-Flying Mach 8 Scramjet

HyShot 6 will use an up-and-down trajectory similar to HyShot 2, but the scramjet engine will separate from the rocket and enter the atmosphere on its own at about Mach 8. It will be a payload of around 250 kg, over twice the size of the HyShot 2 payload. The goal of the flight is to measure actual thrust levels of the scramjet over five seconds of scramjet engine operation. A three-dimensional scramjet flowpath developed at The University of Queensland will be flown.

HyShot 7 – Sustained Mach 8 Scramjet Powered Flight

HyShot 7 is the culmination of the other two flights. It will be a scramjet-powered vehicle and its design will make use of the information learned from HyShot 5 and 6. A depressed trajectory will be used for this flight and the goal is to fly the scramjet-powered vehicle horizontally for up to a minute at Mach 8. The engine structure will reach a thermally steady-state condition in this period, so this flight is a proof-of-concept for long duration scramjet flight.

Preliminary testing of a candidate 3-D scramjet flowpath for HyShot VI has begun in T4. The engine includes a Rectangular-to-Elliptical Shape Transition (REST) inlet (Smart 1999,2001) and a divergent combustor with elliptical cross-section. Figures 20 and 21 show 2 photographs of the shock tunnel model used in the experiments, which was fabricated from high strength plastic. The short duration of the test-time in T4 allows the use of such fabrication techniques, which cannot be used for longer duration testing or flight. Figure 22 shows some preliminary test data for the engine. The test flow conditions were equivalent to Mach 8 flight at 30 km altitude, which corresponds to a dynamic pressure of 0.5 atmospheres, and the fuel was gaseous hydrogen. The bodyside pressure distributions in Fig. 22 indicate a clear pressure rise due to combustion in the combustor and nozzle.

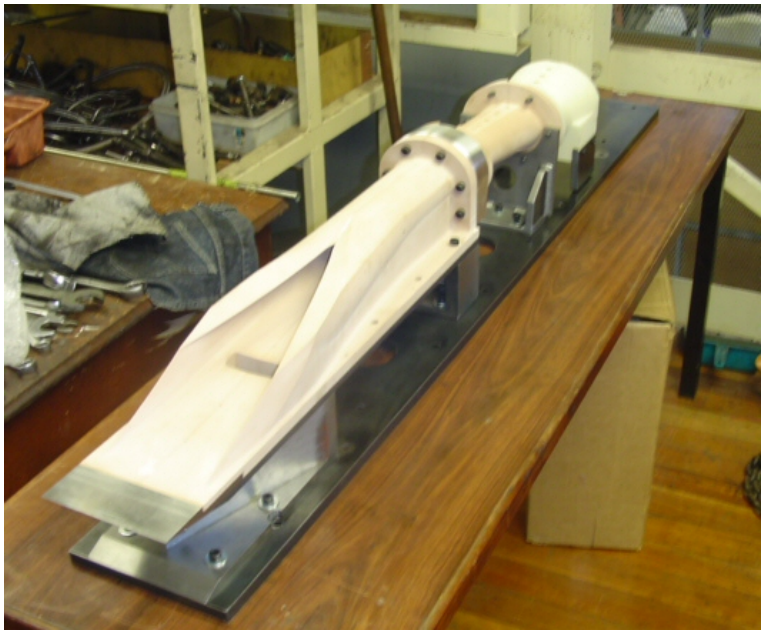

Figure 20: REST engine model for T4.

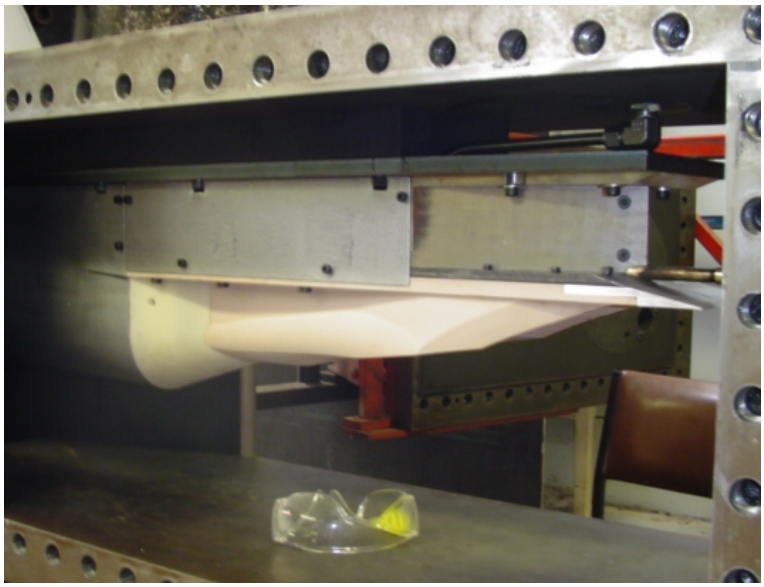

Figure 21: REST engine mounted in the T4 test section.

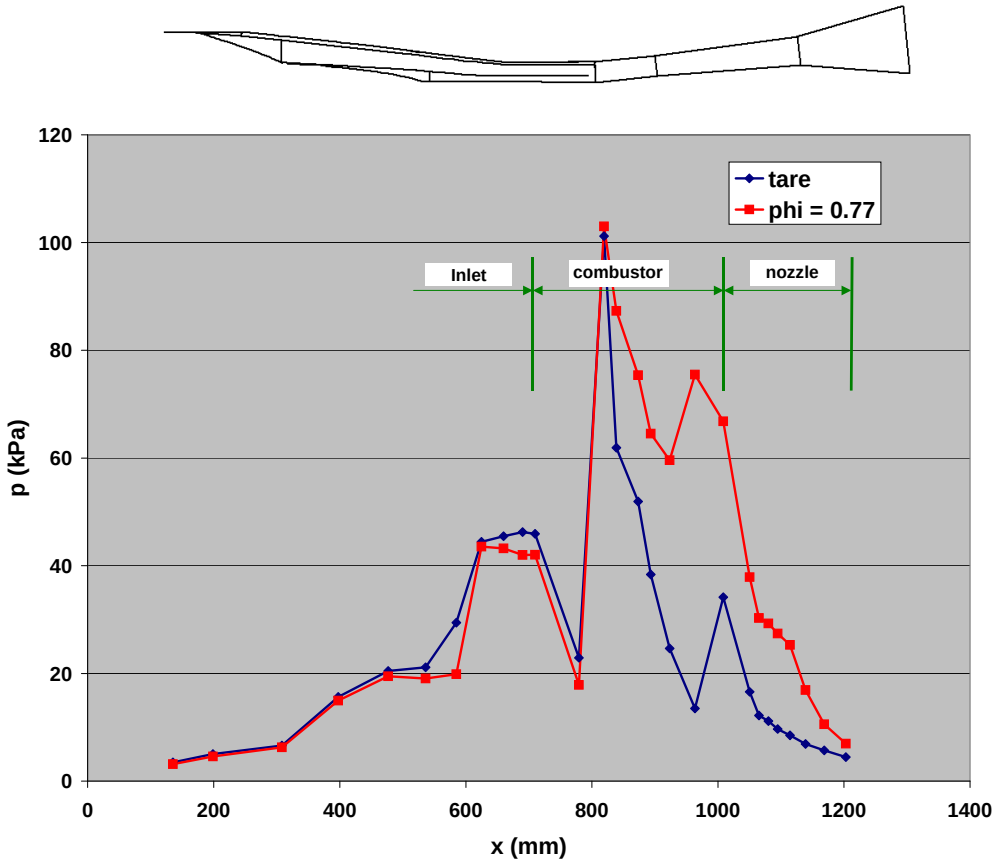

Figure 22: Preliminary REST engine data at Mach 8 (p = duct pressure, x = distance from leading edge of the model, phi = equivalence ratio).

Together with the flight experiments, the Centre for Hypersonics at The University of Queensland will continue to conduct fundamental research on scramjet flowpaths, with particular emphasis on Flight Mach numbers of 10 and above.

11.0 REFERENCES

Brescianini, C., 1993, "An investigation of the wall injected scramjet", PhD thesis, The University of Queensland.

Buttsworth, D.R., 1994, "Shock induced mixing and combustion in a scramjet", PhD thesis, The University of Queensland.

Cain, T., Owens, R. and Walton, C., 2004, "Reconstruction of the HyShot 2 Flight from Onboard Sensors" Fifth Symposium on Aerothermodynamics for Space Vehicles, Cologne, Germany.

Casey, R.T., Stalker, R.J. and Brescianini, C., 1992, "Hydrogen combustion in a hypersonic airstream", Aeronautical Journal, 96(955), p200-202.

Gardner, A.D., 2001, "Upstream porthole injection in a 2-D scramjet model", M.Sc thesis, The University of Queensland.

Goyne, C.P., Stalker, R.J., and Paull, A., 2000, "Hypervelocity skin friction reduction by boundary layer combustion of hydrogen", Journal of Spacecraft and Rockets, 37(6), 740-746.

Hall, N.A., 1951, "Thermodynamics of fluid flow", Prentice Hall, New York, p169-171.

Hayne, M.J., Mee, D.J., Morgan, R.G., Gai, S.L. and McIntyre, T.J. 2003, "Heat transfer and flow behind a step in high enthalpy superorbital flow", The Aeronautical Journal, vol. 109(1073), pp. 435-442.

Hayne, M.J., 2004, "Hypervelocity Flow Over Rearward-Facing Steps", PhD Thesis, The University of Queensland.

He, Y. and Morgan, R.J., 1994, "Transition of compressible high enthalpy boundary layer flow over a flat plate", Aeronautical Journal, 98(972), p25-34.

Huber, P.W., Schexnayder, C.J. and McClinton, C.R., 1979, "Criteria for self-ignition of supersonic hydrogen-air mixtures", NASA TP 1457.

Kovachevich, A., Paull, A. and McIntyre, T., 2004, "Investigation of an intake injected hot wall scramjet", AIAA paper 2004-1037.

McIntyre, T.J., Houwing, A.F.P., Palma, R.C., Rabbath, P.A.B. and Fox, J.S., 1997, "Optical and pressure measurements in shock tunnel testing of a model scramjet combustor", Journal of Propulsion and Power, 13(3), p388-394.

Mee, D.J., Daniel,W.J.T, Simmons, J.M., 1996, "Three-component force balance for flows of millisecond duration", AIAA Journal, 34(3), p590-595.

Morris, N.A., 1989, "Silane as an ignition aid in scramjets", PhD thesis, The University of Queensland.

Odam, J., 2004, "Scramjet experiments using radical farming", PhD thesis, The University of Queensland.

Paull, A., Stalker, R.J., and Mee, D.J., 1995, "Experiments on supersonic ramjet propulsion in a shock tunnel", Journal of Fluid Mechanics, 296, p150-183.

Paull, A., 1996, "A simple shock tunnel driver gas detector", Shock Waves Journal, 6(5), p 309-312.

Paull, A., Frost, M. and Alesi, H., "HyShot-T4 Supersonic Combustion Experiments", report for NAG-1-2113, University of Queensland, 2000.

Paull, A., Alesi, H. and Anderson, S.,2002, "HyShot Flight Program and how it was developed", AIAA 02-4939.

Pulsinetti, M.V., 1997, "Scaling laws for scramjets, PhD thesis, The University of Queensland.

Sanderson, S.R., and Simmons, J.M., 1991, "Drag balance for hypervelocity impulse facilities", AIAA Journal, 29(12), p2185-2191.

Ressler, E.L., and Bloxsom, D.E. 1952., "Very high Mach number flows by unsteady flow principles", Cornell University Grad. Sch. of Aero. Eng, limited distribution monograph.

Skinner, K.A., 1994, "Mass spectrometer of hypersonic combustion", PhD thesis, The University of Queensland.

Smart, M.K., 1999, "Design of Three-Dimensional Hypersonic Inlets with Rectangular-to-Elliptical Shape Transition", Journal of Propulsion and Power, Vol. 15, No. 3, pp 408-416.

Smart, M.K., 2001, "Experimental Testing of a Hypersonic Inlet with Rectangular-to-Elliptical Shape Transition", Journal of Propulsion and Power, Vol. 17, No. 2, pp 276-283.

Smart, M.K., Hass, N.E. and Paull, A., 2006, "Flight Data Analysis of the HyShot 2 Flight Experiment", AIAA Journal, Vol. 44, No. 10, pp 2366-2375.

Stalker, R.J., Morgan, R.G. and Paull, A., 1996, "A shock tunnel investigation of scramjet performance with partially premixed combustion", AIAA paper No. 96-4534.

Stalker, R.J. and Paull, A., 1998, "Experiments on cruise propulsion with a hydrogen scramjet", Aeronautical Journal, 102(1011), p37-43.

Stalker, R.J., Truong, N.K. Morgan, R.G. and Paull,A., 2004, "Effects of hydrogen-air non-equilibrium chemistry on the performance of a model scramjet thrust nozzle", 108(1089), p575-584.

Stalker, R.J., 2005, "Control of hypersonic turbulent skin friction by boundary layer combustion of hydrogen", Journal of Spacecraft and Rockets", 42(4), 577-587.

Tuttle, S.L., Mee, D.J., and Simmons, J.M., 1995, "Drag measurements at Mach 5 using a stress wave force balance", Experiments in Fluid, 19, p336-341.

Tuttle, S.L., 1996, "Measuring thrust and drag in a hypersonic impulse facility", PhD thesis, The University of Queensland.

Wendt, M.N., Jacobs, P.A. and Stalker, R.J., 1999, "Displacement effects and scaling of ducted supersonic flames", Combustion & Flame, 115(4), 593-604.